RNA (1999), *5*:1384–1395. Cambridge University Press. Printed in the USA.

A sulfate pocket formed by three GoU pairs in the 0.97 Å resolution X-ray structure of a nonameric RNA

BENOÎT MASQUIDA, CLAUDE SAUTER, and ERIC WESTHOF

Institut de Biologie Moléculaire et Cellulaire—Centre National de la Recherche Scientifique, UPR 9002 Structure des Macromolécules Biologiques et Mécanismes de Reconnaissance, 67084 Strasbourg, France

ABSTRACT

The crystal structure of the RNA duplex [r(CGUGAUCG)dC]$_2$ has been solved at a resolution of 0.97 Å. The model has been refined to R-work and R-free of 14.88% and 19.54% for 23,838 independent reflections. The base-pairing scheme forces the 5′-rC to be excluded from the helix and to be disordered. In the crystals, the sequence promotes the formation of two GoU wobble pairs that cluster around a crystallographic threefold axis in two different ways. In the first contact type, the GoU pairs are exclusively surrounded by water molecules, whereas in the other contact type, the three amino groups of the guanine residues of the symmetry-related GoU pairs trap a sulfate ion. This work provides the first example of the interaction of a GoU pair with a sulfate ion in a helical context. Despite the negative charge on the polynucleotide backbone, the guanine amino N2 is able to attract negatively charged groups that could, in the folding of complex RNA molecules, belong to a negative phosphodiester group from a neighboring strand and, in a RNA–protein complex, to a negative carboxyl group of an aspartate or glutamate side chain.

Keywords: GoU pair; sulfate ion; synchrotron; X-ray crystallography

INTRODUCTION

Several structures of RNA helices containing GoU pairs have been obtained [for a review, see Auffinger & Westhof (1998)]. The GoU pairs observed in crystals of helices are often accompanied by non-Watson–Crick pairs, like U·U (Baeyens et al., 1995) or U·C pairs (Holbrook et al., 1991). G·A and A·A mismatches have also been observed (Baeyens et al., 1996). Another kind of unexpected feature consists in the slippage in the 5′ direction of one strand of the helix upon crystallization (Biswas & Sundaralingam, 1997). Interestingly, those crystal structures of RNA helices incorporating mismatches were obtained upon crystallization of sequences designed with the hope of observing tetraloops at high resolution. Such small single-stranded hairpin motifs are in dynamic equilibrium with intermolecular double-stranded helices incorporating necessarily base mismatches. Apparently, despite the noticeable thermal stability of the closing tetraloops (Antao & Tinoco, 1992), crystal assembly and packing drive the equilibrium toward double-stranded helices and non-Watson–Crick base pairing instead of hairpin motifs.

A rearrangement of the base-pair scheme due to the slippage of one strand in the 5′ direction led to the formation of a Watson–Crick paired double helix with two GoU pairs in the RNA structure presented in this paper. Crystals were obtained while attempting to crystallize the 4-nt sequence 5′-UGAU-3′, responsible for the most determining structural feature of the 3′-untranslated region of eukaryotic selenoprotein messengers (Walczak et al., 1996, 1998). The crystal structure of the resulting nonameric RNA 5′-rCGUGAUCGdC has been solved and refined at a resolution of 0.97 Å.

GoU pairs have a prominent role in RNA–RNA recognition [e.g., the wobble interaction in the anticodon–codon triplets (Crick, 1966)] and in RNA–protein complex formation [e.g., tRNA^{Ala} (Park et al., 1989)]. Besides, in some catalytic RNA [group I intron (Cech et al., 1981) or the hepatitis delta virus ribozyme (Sharmeen et al., 1988)], a GoU pair is present at the cleavage site. For group I introns, specific contacts in the shallow groove of the GoU pair have been proposed (Michel & Westhof, 1990) and experimentally determined (Strobel &

Reprint requests to: Eric Westhof, Institut de Biologie Moléculaire et Cellulaire—Centre National de la Recherche Scientifique, UPR 9002 Structure des Macromolécules Biologiques et Mécanismes de Reconnaissance, 15 rue René Descartes, 67084 Strasbourg, France; e-mail: westhof@ibmc.u-strasbg.fr.

Ortoleva-Donnelly, 1999). In the crystal structure of the P4–P6 domain of the group I intron of *Tetrahymena thermophila*, the deep groove of tandem GoU pairs binds magnesium ions as well as osmium- or cobalt-hexamine (Cate & Doudna, 1996). Thus, the binding of magnesium ions by RNA constitutes an example of the incorporation of nonnucleic acid components in a sequence specific manner. Nevertheless, the binding of magnesium ions in the deep groove of GoU pairs does not involve the N2 amino group of the guanine (situated in the opposite groove). Here, we present a crystal structure in which GoU pairs, clustered around a crystallographic axis, interact with a sulfate dianion. Because sulfate and phosphate anions are structural analogs, GoU pairs could help in the folding of complex RNA molecules by interacting with the phosphate group of single strands in the shallow groove side. Further, in RNA–protein complexes, negatively charged protein side chains could also bind to the amino group of guanines in shallow grooves.

RESULTS

Sequence is an important screening parameter in RNA crystallization (Scott et al., 1995; Anderson et al., 1996). We have, therefore, tested three different self-pairing oligoribonucleotides sharing the sequence 5′-UGAU-3′ (Sec1: 5′-G**UGAU**C-3′; Sec2: 5′-GC**UGAU**GCdC-3′; Sec3: 5′-CG**UGAU**CGdC-3′). Only the Sec3 sequence gave crystals suitable for crystallographic studies.

The RNA crystallizes in space group R3 with unit cell dimensions $a = b = 39.9$ Å, $c = 67.4$ Å, and $\gamma = 120°$ in the hexagonal setup. The asymmetric unit consists of a duplex of 8 bp with a disordered 5′-rC, a sulfate ion, and 84 water molecules (Table 1). The base-pair scheme consists of four central Watson–Crick pairs, two G=C and two A—U, with a GoU pair on each side. Finally, a G=C pair closes each end of the duplex. The resulting dangling 5′ rC is not observed in the density (Figs. 1A and 2A), as recently observed in a crystal structure of a DNA–RNA hybrid (Xiong & Sundaralingam, 1998).

TABLE 1. Data collection and model refinement statistics.

X-ray source	IBMC-ESRF ID14/EH4[a]
λ (Å)	1.5418, 0.9384
Number of crystals	2
Space group	R3
Lattice parameters (Å)	$a = 39.958$; $c = 67.445$
Resolution (Å)	20–0.97 (0.99–0.97)[b]
Rsym (%)	4.1 (44.6)
Number of observations	140,902
Number of unique reflections used in refinement	23,838
Completeness (%)	99.8 (99.9)
$<I/\sigma_I>$	22.6
R-factor/R-free (%)	14.88/19.54
Number of atoms (RNA/ion/solvent)	342/5/84
RMS bond lengths (Å)	0.014
RMS angle distances (Å)	0.018

[a]The high resolution data sets from the ESRF were merged with a low resolution pass collected on an in-house Enraf-Nonius generator.
[b]The last shell is indicated by parentheses.

Overall description of the structure

The duplex is right handed and all the torsion angles are in the usual range for A-form RNA. A torsional change occurs at the G4–A5 step in one of the strands forming the duplex where A5 has α/γ angles shifted from the most frequent *gauche*$^-$/*gauche*$^+$ to the less frequently observed *trans/trans* conformation. Nucleotide A5 makes two intermolecular contacts (see Fig. 5) and, thus, crystal packing might be responsible (at least partially) for the *trans/trans* conformation at G4–A5 step. The UoG pairs are sandwiched between two G=C pairs. The majority of stacking interactions occurs between consecutive intrastrand residues. Nevertheless, GoU pairs break the stacking continuity. Interstrand stacking, known to occur in RNA at 5′-γR-3′ steps, is emphasized with GoU pairs (Fig. 1B) (Mizuno & Sundaralingam, 1978). The first 4 bp of the duplex are related to the last 4 by a noncrystallographic twofold axis perpendicular to the crystallographic threefold axis.

Packing interactions

The duplexes form in head-to-tail fashion pseudo-infinite columns which pack together through backbone–

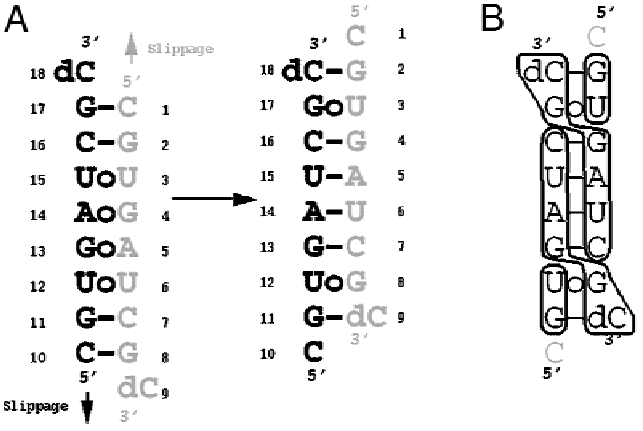

FIGURE 1. Secondary structure of Sec3 oligoribonucleotide. **A**: The expected base-pair scheme that should take place in the full-length selenocysteine insertion sequence motif is rearranged to the observed base-pair scheme by slippage of 2 bp in the 5′ direction. The stretch of noncanonical base pairs, U·U, G·A, A·G, U·U does not occur and two GoU pairs are consequently formed. **B**: The stacking continuity (framed nucleotides) is interrupted by the GoU pairs, G of the GoU stacks on the G of the following C=G pair on the other strand. One side of U3, C7, U12, and C16 is thus more exposed to the solvent than in the other residues.

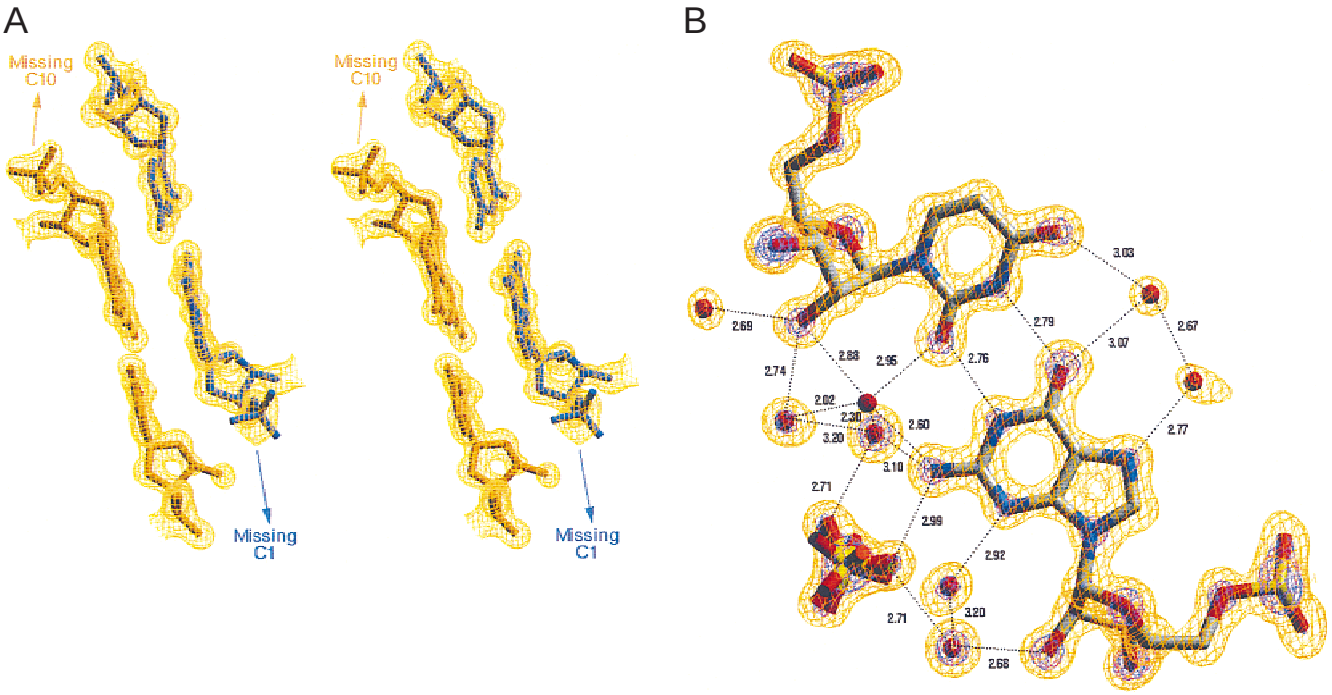

FIGURE 2. **A**: Stereo side-by-side view of the contact region between two stacked duplexes (orange and blue). The low twist value increases the stacking interactions. The 2 σ contoured ($2F_{obs} - F_{calc}$) map shows that the phosphate groups at the 5′-ends are present. The anchor points of the disordered 5′-rC, numbered 1 and 10, are indicated by a blue and an orange arrow, respectively. According to the B-factors, the phosphate group of C1 appears less ordered than the phosphate group of C10. **B**: The GoU pair of the sulfate pocket is represented with the network of water molecules in the deep and shallow grooves. All atoms contribute to the electronic density in a ($2F_{obs} - F_{calc}$) map contoured at 2.5 σ (orange). The individualization of the atoms is also characteristic of high-resolution structures. When the contour level is raised to 4 σ, only atoms heavier than carbon are still seen (purple). The water molecule showing no electronic density associated is a low occupancy site, W174.

backbone interactions taking place between symmetry-related duplexes (see below). At the step between two stacked duplexes, the twist angle is low (16.95°), as observed in the two crystal structures of 8-bp duplexes solved in R3 (Wahl et al., 1996; Biswas et al., 1997). Strikingly, the 5′-rC is not observed in the electronic density; however, its presence has been assessed by mass spectrometry (see Materials & Methods). Moreover, the phosphate group of G2 and G11 are clearly seen indicating that the 5′-cytidine is not lost. Alkaline hydrolysis would have produced 5′-hydroxyl G instead of phosphorylated ones. The 5′-cytidine is thus disordered (Fig. 2A).

Each wobble pair participates in the packing by clustering around the threefold axis in two distinct manners. In the first contact (G17oU3), the N2 amino group of the G contacts one oxygen atom of a sulfate ion. The sulfur atom is located on the threefold axis, but is not oriented so as to satisfy the threefold symmetry, that is, with an oxygen atom along the axis. In fact, two oxygen atoms belong to the plane perpendicular to the threefold axis with the remaining oxygen atoms placed above and below the plane at 1.2 Å of the axis. Three conformers of the sulfate are, thus, present on the threefold axis (Fig. 2b). The sulfate ion is bonded to three water molecules (W103, W105; W145, not located in the plane of the GoU pair, is only depicted in Fig. 3A). Packing interactions are strengthened through van der Waals contacts between the ribose moieties of the threefold related GoU pairs (Fig. 3A). In the second contact (G8oU12), the three symmetry-related 2′-OH groups of G point towards a water molecule located on the threefold axis (Fig. 3B). The relation of G8 to the threefold axis results in the location of U12 at a remote distance from the crystallographic axis. As a consequence of the packing, two sulfate ions are positioned on the same crystallographic axis only in noncontiguous layers of RNA duplexes (Fig. 4).

Three types of RNA–RNA packing contacts are observed (Fig. 5A). The 2′-hydroxyl group of A5 forms one hydrogen bond with the O1P atom of G4 in a symmetry-related duplex. The same type of contact is observed between the 2′-hydroxyl residue G11 and the O1P atom of residue dC18 of another symmetry-related duplex. A third type involves the 2′-hydroxyl group of G17 with the N2 atom of G2.

Hydration of the duplex

The duplex is hydrated by 84 clearly identified water molecules. Among these, seven are located at special positions with an occupancy of one third. Sixteen other

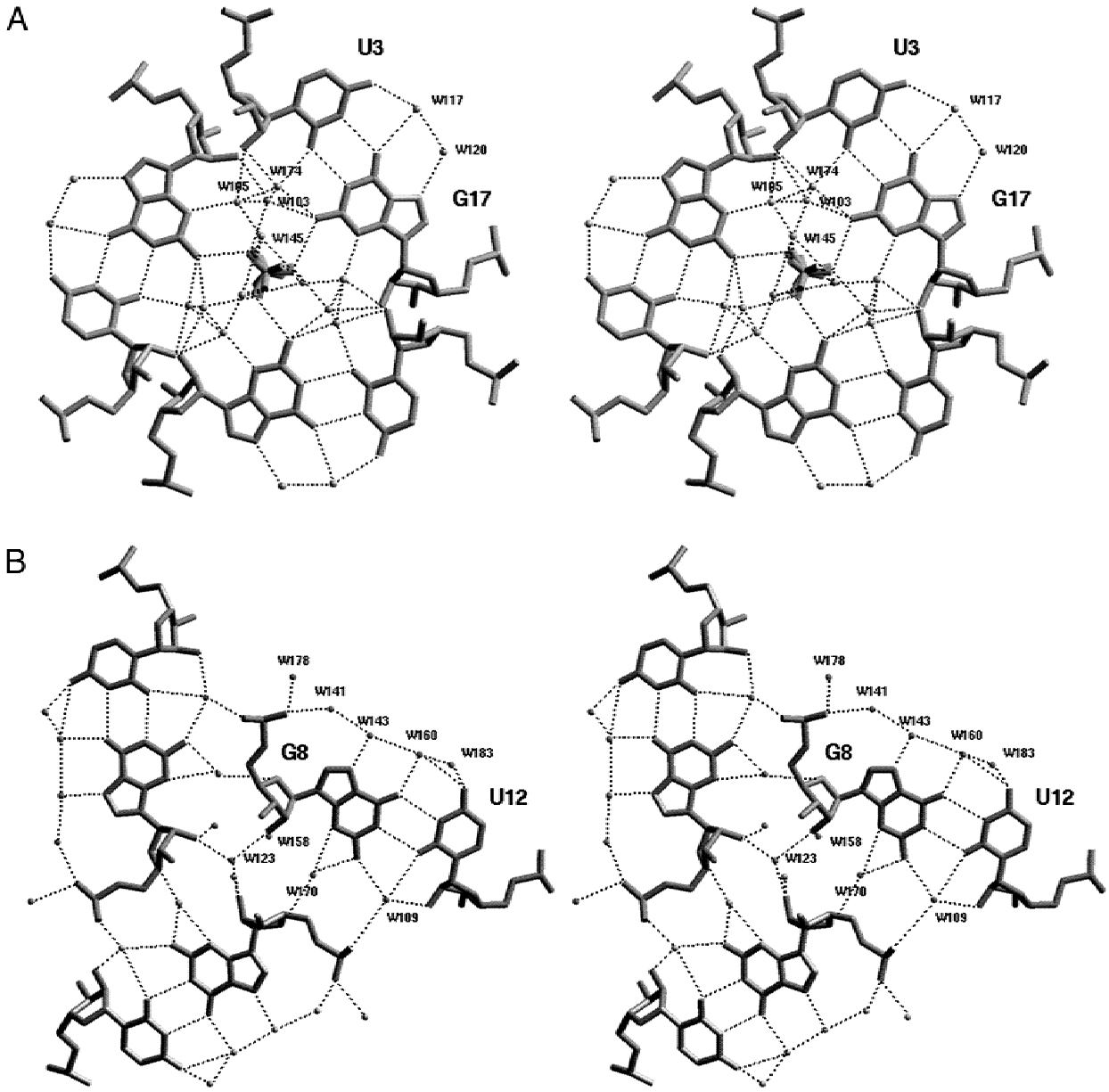

FIGURE 3. Side-by-side stereo drawings of symmetry-related GoU pairs that cluster in a propeller twist fashion in two different ways around the threefold axis. **A**: The sulfate ion located on the axis is trapped by three GoU pairs that contact directly the ion with the N2 amino group of the G residues. Three water molecules also interact directly with the ion. Symmetry operations raise the number of hydrogen bonds from four in the asymmetric unit to 12. It is worth noting that the riboses of the GoU pairs perform van der Waals contacts with riboses of the symmetry-related GoU pairs. **B**: A water molecule located on the threefold axis interacts with the 2′-OH groups of the three symmetry-related G residues participating in the GoU pair. The U residues are thus located far away from the axis and face the shallow groove of another duplex. Only the water molecules and the nucleotides from the asymmetric unit are labeled for clarity. All hydrogen bonds drawn imply a distance between heavy atoms of between 2.3 and 3.5 Å.

solvent molecules are linked with intermolecular distances below 2.4 Å and occupancies of 0.50. W174 interacts with U3, which is involved in one of the GoU pairs trapping the sulfate ion. The close proximity of the very well-defined sites W103 and W105–W174 indicates that the latter has a low occupancy (0.20) coupled to the occupancies of W103 (0.95) and W105 (0.85) (Fig. 3A). Seventy-eight hydration sites belong to the first hydration shell and six to the second (W111, W154, W162, W168, W176, and W182). An average of 10.5 water molecules per base-pair step is observed, in agreement with other high-resolution RNA structures (for reviews, see Egli et al., 1996; Auffinger & Westhof, 1998; Masquida & Westhof, 1999).

Four water molecules (W101, W104, W123, and W133), because of their location on the threefold axis, are bound to oxygen atoms of three symmetry-related duplexes simultaneously. This occurs for the 2′-OH of

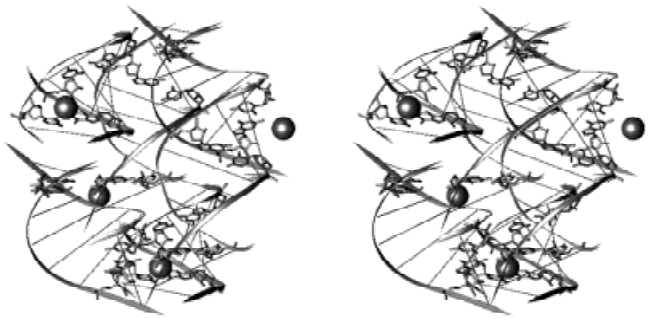

FIGURE 4. Two layers of duplexes related by symmetry operations without translation (x, y, z; $-y, x-y, z$; $y-x, -x, z$). Helices are represented by two ribbons linked by bars symbolizing base pairs. GoU pairs are drawn in ball & stick. The sulfate ion is drawn as a large sphere to emphasize its location in the packing. All spheres are crossed by a colinear threefold axis orientated along the helical axis. Two sulfate ions are located on the same threefold axis only when belonging to noncontiguous RNA duplex layers.

G4, 3′-OH of 3′-dC18, 2′-OH of G8, and for the O1P atom of A5. Most of these residues are also involved in direct RNA–RNA interactions. The sulfate ion is, thus, locked in a tight pocket and in direct contact with three different water molecules (W103, W105, and W145) in addition to the N2 atom of G17 (Fig. 3A). Those three water molecules form a hydration cone centered around the S-O2 bond of the sulfate ion. W103 bridges the N2 atom of G17 to the 2′-OH group of a symmetry-related G17. W105 is bound to the 2′-OH of U3 and contacts the N3 atom of a symmetry-related G17. W145 does not contact tightly any RNA atom of the pocket (the distance W145(O2′(G4) is 3.21 Å), but is close to the sulfate ion (the distance W145…O4(SO_4) is 2.47 Å). All three water molecules interact with some other water molecules and RNA groups in the shallow groove. Some differences in the resulting hydration patterns of the shallow grooves of GoU pairs are, however, worth noting. In the sulfate trap, the water site linking the amino group of the G to the O2 and O2′ atoms of the U (W174) has an occupancy of 0.20. This site, described as characteristic of GoU pairs, is thus underpopulated in the GoU pair surrounding the sulfate ion. Although the hydration patterns of the GoU of the sulfate trap diverge from the hydration pattern canonically observed for GoU pairs, the network of water molecules in the region around the second GoU pair (G8oU12) is in agreement with previously reported structures (Auffinger & Westhof, 1998; Mueller et al., 1999).

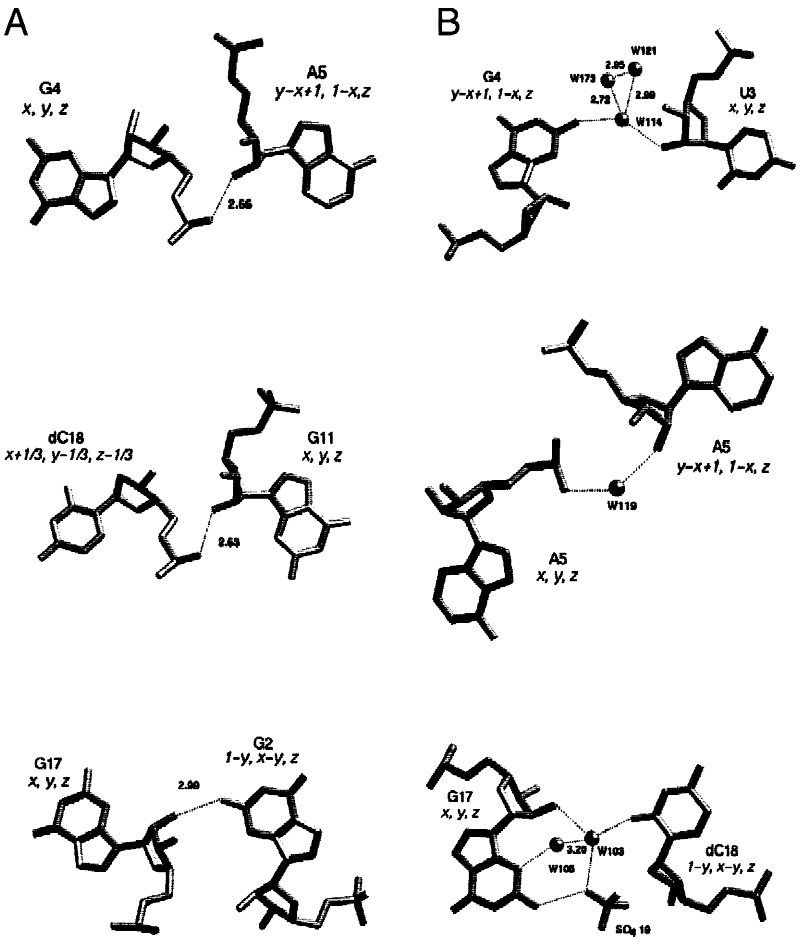

FIGURE 5. Intermolecular contacts observed in the structure. **A**: Direct RNA–RNA contacts involve the O1P atom of one nucleotide together with the O2′ group of its partner. G17, involved in the sulfate binding, makes a contact with G2 that closes the pocket of the sulfate ion on one side. **B**: Several residues are involved in water-mediated RNA–RNA contacts with other residues in their vicinity, thus widening the contacting zone.

Thus, it seems that the presence of the sulfate ion induces a perturbation of the hydration scheme of the GoU pairs.

The other water molecules are mainly involved in interstrand interactions within a given duplex or between symmetry-related ones (Fig. 5B). The step between two stacked duplexes shows optimized stacking interactions between G2 and G11. Moreover, two water molecules pinch the interduplex step in both the deep and shallow grooves. W106 bridges the N3 atom of G3 to the N2 atom of G11, and W130 bridges the O6 atoms of these residues. The diversity of contacts mediated by water molecules can be subdivided into categories very commonly observed in RNA structures, assessing the correctness of the network of water molecules we observe in the present structure (for review, see Westhof & Beveridge, 1990). The first category of water bridges is formed between atomic groups usually involved in the ribose zipper, that is, the O2 atom of a pyrimidine (or the N3 atom of a purine) with a 2′-OH group of a symmetry-related duplex ((C18*) O2…W103…O2′ (G17), (G4) N2…W114…O2′ (U3*)) (Cate et al., 1996; Auffinger & Westhof, 1997). Sometimes, the contact involves an anionic oxygen atom of a phosphate group ((A5) O2′…W119…O2P (A5*), (A5) N3…W173…O1P (G4*)). The second category connects interstrand atoms of the bases ((U6) O2… W116…O2 (U15)). The third category involves phosphate bridges between consecutive residues on the same strand (G17(O1P)…W125…dC18(O2P)). Finally, the base of a single nucleotide can be bridged to the ribose–phosphate in the deep groove ((G13) O2P… W122…N7 (G13)) or in the shallow groove ((A14) N3…W115…O2′ (A14), (G4) N3…W108…O2′ (G4)).

The deep groove of the duplex is very well hydrated. However, the global hydration network is sometimes interrupted by a distance greater than 3.5 Å between water molecules or by RNA–RNA contacts (Fig. 6). The distances (below 3.5 Å) between any atom of the RNA or the sulfate ion and the water molecules are reported in Table 2.

DISCUSSION

In this work, we describe the structure of a nonameric RNA obtained at 0.97 Å of resolution and containing six Watson–Crick and two GoU wobble pairs. The latter are formed in two distinct structural contexts. Whereas one of them is hydrated as previously observed (for review, see Auffinger & Westhof, 1998), the second one constitutes the first reported RNA-binding site for a sulfate ion in a helical context. Protein structures in which a sulfate ion is bound show that a protein pocket can hold a sulfate ion solely by a set of hydrogen bonds (often with side chains of Asn residues), as in the sulfate-binding protein of *Salmonella typhimurium* (Pflugrath & Quiocho, 1985) or in the satellite of the tobacco mosaic virus crystal structure (Larson et al., 1998). The hydrogen-bonding network is sometimes reinforced by several salt bridges, as in the human theta class glutathione transferase (Rossjohn et al., 1998). The network of solvent molecules in contact with the sulfate ion could be water molecules or ammonium ions. However, in the present case, the observed number of 12 hydrogen bonds is consistent with a coordination of the ion purely formed by hydrogen-bond donors such as amino groups or water molecules.

The basis for the biological role of GoU pairs has been emphasized in the crystal structure of the P4–P6 domain of the group I intron of *Tetrahymena* (Cate et al., 1996). The deep groove of tandem GoU pairs binds magnesium ions that can be replaced under special conditions by a variety of metal ions like osmium- or cobalt-hexamine (Cate & Doudna, 1996). Here, we present a crystal structure in which a sulfate dianion interacts in the shallow groove of three GoU pairs, clustered around the crystallographic axis. Although the presence of the sulfate ion is obviously due to the crystallization conditions, its ability to bind to GoU pairs is somehow puzzling. An octameric RNA (Portmann et al., 1995) has been recently crystallized in conditions containing ammonium sulfate. The space group (R32) together with the lattice parameters make the

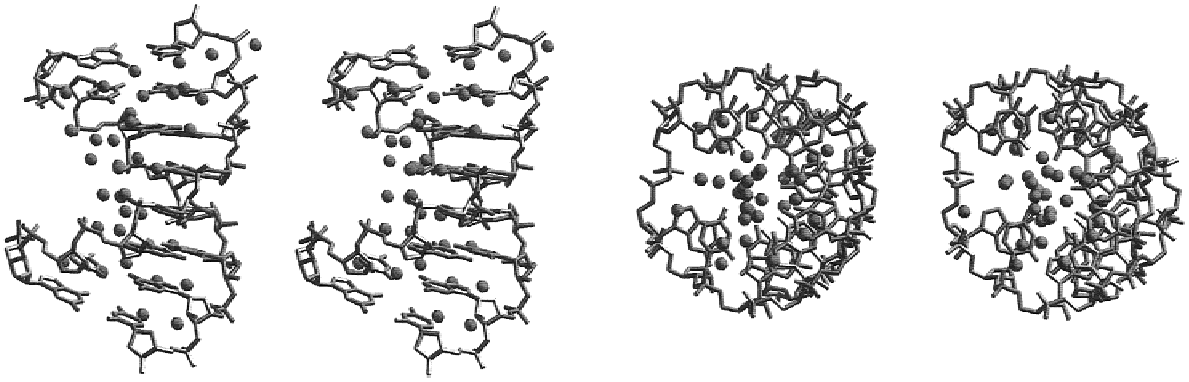

FIGURE 6. Side-by-side stereo representation of the hydration of the deep groove of the duplex. Three to five water molecules interact with the deep groove sites of each pair.

TABLE 2. Distances between non-hydrogen RNA atoms (A) or sulfate ion (B) and water molecules. The O1P and O2P atoms correspond to O_S and O_R oxygens of the phosphate groups, respectively. The symmetry operation is not indicated when both heavy atoms belong to the same asymmetric unit.

A. Distances between non-hydrogen RNA atoms and water molecules

Strand 1				Strand 2			
(Residue) atom type	Symmetry operation	Water number	Distance (Å)	(Residue) atom type	Symmetry operation	Water number	Distance (Å)
(G2) O2P		W181	2.96				
2(G2) O5T		W163	2.35	(G11) O5T	$y - x + 2/3, -x + 1/3, z + 1/3$	W110	2.68
				(G11) N2	$x - 1/3, y - 1/3, z - 1/3$	W106	2.91
(G2) N3	$1 - y, x - y, z$	W106	2.91	(G11) N3	$x - 1/3, y - 1/3, z - 1/3$	W106	3.49
(G2) O6		W120	3.08	(G11) O6	$y - x + 2/3, -x + 1/3, z + 1/3$	W130	3.01
		W130	2.96				
(G2) N7		W124	2.88	(G11) N7		W175	2.84
(G2) O2′		W137	2.84	(G11) O2′	$x - 1/3, y - 1/3, z - 1/3$	W110	2.84
(U3) O1P		W166	2.81				
(U3) O2P		W155	3.33				
(U3) O2		W174	2.95	(U12) O2		W109	3.29
(U3) O4		W149	3.32	(U12) O4		W160	3.33
		W124	3.47			W183	2.68
		W120	3.03			W144	3.25
(U3) O2′		W114	2.69	(U12) O2′		W109	2.76
		W105	2.74				
		W174	2.88				
(G4) O1P		W131	3.00				
		W173	2.89				
		W171	2.80				
(G4) O2P		W146	2.73	(G13) O2P		W122	3.02
		W155	2.69			W180	2.57
(G4) N3		W108	2.84	(G13) N3		W126	2.93
(G4) N2	$1 + y - x, 1 - x, z$	W114	2.80				
(G4) O6		W149	2.72	(G13) O6		W144	2.74
(G4) N7		W134	2.87	(G13) N7		W122	2.85
(G4) O2′	$1 + y - x, 1 - x, z$	W145	3.21	(G13) O2′		W159	2.71
		W101	2.86				
		W108	2.69				
	$1 + y - x, 1 - x, z$	W145	3.21				
(A5) O1P	$1 - y, x - y, z$	W148	3.14				
		W133	2.59				
(A5) O2P		W118	2.64	(A14) O2P		W180	3.09
		W119	2.85				
(A5) N3	$1 + y - x, 1 - x, z$	W131	3.24	(A14) N3		W115	2.97
	$1 + y - x, 1 - x, z$	W173	2.55				
(A5) N6		W161	3.24	(A14) N6		W172	2.95
(A5) N7		W156	2.91	(A14) N7		W138	2.74
(A5) O2′	$1 + y - x, 1 - x, z$	W119	2.92	(A14) O2′		W115	2.82
	$1 + y - x, 1 - x, z$	W173	3.29			W102	2.79
(U6) O1P		W148	2.84	(U15) O1P		W107	2.80
		W184	2.72			W127	2.89
(U6) O2P		W147	2.82	(U15) O2P		W112	2.87
		W140	2.66			W136	2.77
(U6) O2		W116	2.80	(U15) O2		W116	3.37
(U6) O4		W157	2.84	(U15) O4		W152	2.41
(U6) O2′		W129	2.71				
		W167	2.73				
(C7) O2P		W147	2.92	(C16) O2P		W139	2.53
		W184	3.40			W169	2.75
				(C16) O2		W121	3.10
(C7) N4		W135	2.85	(C16) N4		W164	3.46
				(C16) O2′		W121	2.73
(G8) O1P		W142	3.20	(G17) O1P		W125	2.77
		W113	2.54				

continued

TABLE 2. *Continued*

A. Distances between non-hydrogen RNA atoms and water molecules (continued)

Strand 1				Strand 2			
(Residue) atom type	Symmetry operation	Water number	Distance (Å)	(Residue) atom type	Symmetry operation	Water number	Distance (Å)
(G8) O2P		W178	3.13	(G17) O2P		W128	2.95
		W141	2.74				
(G8) N3		W170	3.06	(G17) N3	$1 + y - x$, $1 - x$, z	W105	2.92
(G8) N2		W109	2.87	(G17) N2		W174	2.60
		W126	3.15		$1 - y$, $x - y$, z	W103	3.10
		W170	2.67				
(G8) O6		W160	2.62	(G17) O6		W120	3.07
(G8) N7		W143	2.50	(G17) N7		W117	2.77
						W179	3.41
(G8) O2′		W123	2.78	(G17) O2′	$1 + y - x$, $1 - x$, z	W174	3.48
		W158	2.53			W103	2.68
(C9) O1P		W153	2.70	(C18) O1P		W106	2.82
						W150	2.87
				(C18) O2P		W128	2.92
(C9) O2P	$y - x + 2/3$, $-x + 1/3$, $z + 1/3$	W181	3.39			W125	2.81
		W165	2.71			W150	3.39
				(C18) O2	$1 - y$, $x - y$, z	W103	2.80
(C9) N4		W151	2.99	(C18) N4		W117	3.49
						W132	2.86
				(C18) O3′		W104	2.66
						W110	2.73

B. Distances between sulfate ion and water molecules

($SO_4$19) O1		W103	2.84
($SO_4$19) O2		W105	3.20
	$1 - y$, $x - y$, z	W145	3.05
	$1 + y - x$, $1 - x$, z	W103	2.71
		W174	3.40
($SO_4$19) O3	$1 - y$, $x - y$, z	W103	2.97
($SO_4$19) O4	$1 + y - x$, $1 - x$, z	W105	3.30
	$1 - y$, $x - y$, z	W145	3.39
		W145	2.47
	$1 + y - x$, $1 - x$, z	W145	2.83

packing in both structures very similar. The region corresponding to the cluster of GoU pairs trapping the sulfate ion in the present structure is replaced in the related structure by a cluster of three G=C pairs with the accompanying network of water molecules (Fig. 7). The comparison between these structures clearly indicates that the N2 groups of the G residues are closer to the threefold axis when belonging to a GoU pair (3.6 Å) than when belonging to a G=C pair (4.9 Å). The resulting narrowing of the hydration channel could be invoked to enable the trapping of the ion. Since sulfate and phosphate are structural analogs, one can expect that guanine amino groups could intervene in the folding of complex RNA molecules through binding of a phosphodiester in the shallow groove of helices. Such an interaction has been observed in a recent crystal structure of an RNA pseudoknot (Su et al., 1999). The O2P atom of a phosphate group from a single-strand junction interacts with the G amino group of a G=C pair in exactly the same fashion as the sulfate ion does with the GoU pair in the present structure (Fig. 8). The topology of the pseudoknot forces a single strand to pass in the shallow groove of a helix and leads to a contact between a phosphate with the N2 group of a G. Thus, the guanine N2 positions seem to constitute favorable and specific binding sites for negatively charged groups. More generally, it seems reasonable to suggest that negatively charged amino acid side chains such as Asp or Glu could interact with the amino group of guanines to mimic the described interaction.

GoU pairs isolated in a Watson–Crick helix adopt characteristic twist values with the preceding and following base pairs in such a way that the step 5′ of the U is overtwisted (compared to the usual 33° value) and the step 3′ of the U undertwisted. We have therefore compared the values in our structure to values in two other high-resolution crystal structures of RNA duplexes containing GoU pairs (Lietzke et al., 1996; Shi

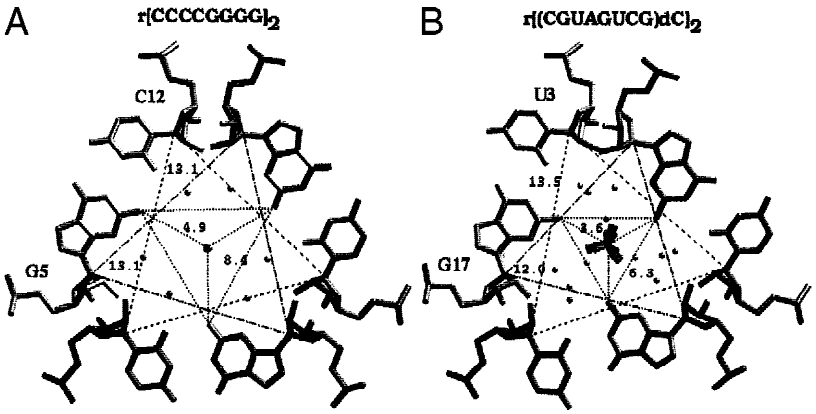

FIGURE 7. Comparison between the crystal structures of (**A**) r(CCCCGGGG)$_2$ (Portmann et al., 1995) and (**B**) the one of the present work. The regions of the packing where ribose rings of symmetry-related duplexes are interacting through van der Waals contacts are depicted. The narrowing of the hydration channel leading to the binding of the sulfate ion to the amino groups of the guanines is clearly seen. Distances between C1′ atoms and between amino groups of symmetry-related residues as well as the distance of the amino group to the crystallographic axis are indicated in angstroms.

et al., 1999). We have also refined *ab initio* models of the duplexes depicted in the crystal structures with NUCLIN/NUCLSQ (Westhof et al., 1985) to check if the observed trend was purely geometric or due to stacking (and possibly to crystal packing). The values presented in Figure 9 show that the effect of the packing is negligible, as average values of crystal and modeled structures are very similar. The same sets of values and trends are obtained upon least-squares geometrical and stereochemical refinement of standard RNA helices (Arnott et al., 1973). Thus, the 5′ high-U-low 3′ twist alternation has essentially a geometric origin stemming from the nonisosteric nature of GoU pairs. On the basis of a crystal structure containing one GoU pair, Mueller et al. (1999) concluded that there is no recognizable structural distortion of the helical fragment away from the wobble pair. In Figure 10, we have superimposed the C1′ atoms of a GoU and a UoG pair at the base of two helical fragments to illustrate the propagation of the high versus low twist angles. Deviations up to 2 Å between the two helices can be observed 5 bp away from the two nonisosteric wobble pairs.

In *Escherichia coli* tRNA^{Ala}, there is a large difference in aminoacylation efficiency between a G3oU70 and a U3oG70 pair (McClain et al., 1988; Musier-Forsyth et al., 1991; Frugier & Schimmel, 1997), leading to the suggestion that the protruding orientation of the 2-amino group is important. As illustrated in Figure 10, if a synthetase locks in the GoU pair via the guanine amino group, a reversal of the GoU pair into a UoG could reorient the -CCA 3′ end in a sufficiently off-track direction to hamper aminoacylation.

Finally, the present crystal structure illustrates the context dependence of small RNA motif consisting of noncanonical base pairs. The NMR determinations of two fragments of the crystallized P4–P6 domain (Cate et al., 1996) present two examples of local structural rearrangements; one in the tetraloop receptor, the internal J6a/b loop (Butcher et al., 1997), and one in loop L5c (Wu & Tinoco, 1998). Interestingly, in both cases, phylogenetic analyses, which reflect the structurally related functional constraints on sequences, identified the correct junctions linking the secondary structure elements (Michel et al., 1982; Cech et al., 1994).

MATERIALS AND METHODS

Synthesis and purification

The nonamer was produced at a 5 μmol scale using phosphoramidite chemical synthesis on an automated DNA/RNA synthesizer (Applied Biosystems, model 392) with a specially dedicated program (Oubridge et al., 1994; Kyoshi Nagai, pers. comm.). A dC residue was added at the 3′ end to promote

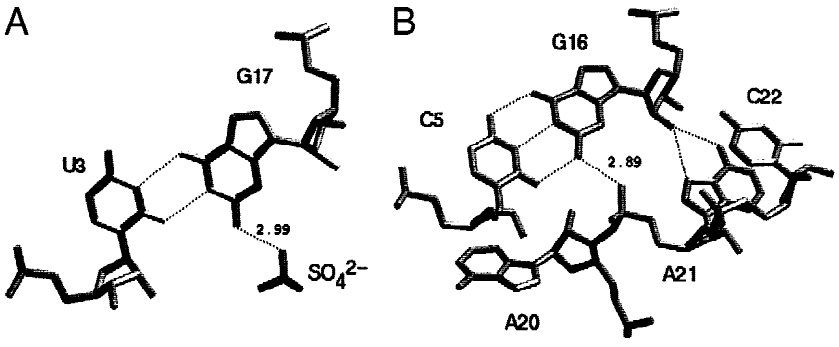

FIGURE 8. A: View of the interaction between the sulfate ion and the N2 group of the G residue involved in the GoU pairing in the present crystal structure. **B**: The possibility for amino groups of guanines to interact with negatively charged groups is exemplified by the crystal structure of a frameshifting RNA pseudoknot (Su et al., 1999) in which an N2 group of a guanine of a G=C pair interacts with the phosphate group of the backbone of the single strand topologically forced to pass in the shallow groove of the helix.

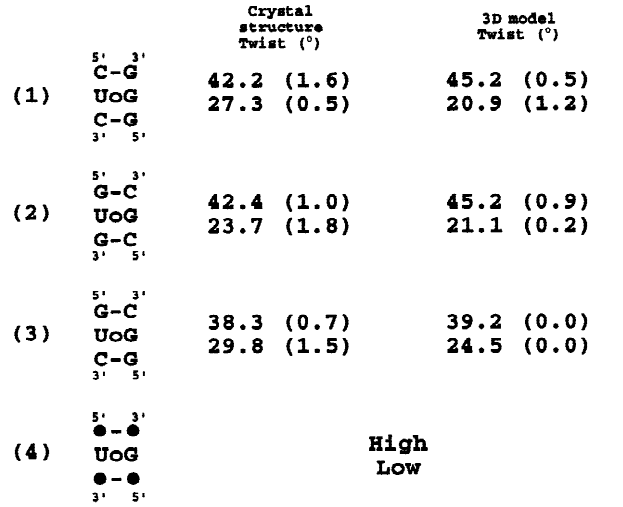

FIGURE 9. Twist values (°, standard deviations indicated by parentheses) at different UoG steps in various Watson–Crick contexts, computed with the program CURVES (Lavery & Sklenar, 1989). The first set of values (left column) is calculated with crystal structures containing isolated UoG pairs: (1) Shi et al., 1999, (2) the present work, (3) Lietzke et al., 1996. The values (second column) stay in the same ranges when computed from ab initio models with the corresponding sequences refined geometrically with NUCLIN/NUCLSQ (Westhof et al., 1985). (4) The twist value is thus higher on the 5′ side than on the 3′ side of the U of the UoG.

intermolecular contacts between symmetry-related molecules as observed elsewhere (Cruse et al., 1994). yet, the presence of the 3′ dC promoted the slippage of one strand in the 5′ direction, resulting in a significant stabilization of the canonical base-pair scheme away from the mismatched one. The RNA was then cleaved from the support and deprotected directly in the column by flowing 8 mL of a mixture of NH_4OH/MeOH (3:1) at regular time intervals during 24 h at room temperature. The solution was filtrated and evaporated to dryness in a speedvac concentrator. Millipore water (250 μL) was added to the pellet to help it dissolve in 8 mL of tetrabutylammonium fluoride (TBAF) 1.0 M in THF, which reacted during 24 h to complete the deprotection of the 2′-hydroxyls. At the end of the reaction, 40 mL of butanol and 0.3 M sodium acetate were added to the solution and stored at −20 °C. The pellet was separated from the liquid phase and dissolved in 20 mL of Millipore water. The quality of the synthesis was assessed by anion-exchange HPLC (Nucleopac-PA-100; DIONEX) using a salt gradient with solutions A (1 mM $NaClO_4$, 20 mM MES, pH 6.2, 4 M urea) and B (400 mM $NaClO_4$, 20 mM MES, pH 6.2, 4 M urea) with 15–70% of solution A over 48 min. Finally, 200 ODs of RNA were loaded on the column to perform a preparative scale purification. The fractions containing the product of correct length were desalted by gel filtration (NAP 25 Pharmacia prepacked column) and evaporated to dryness.

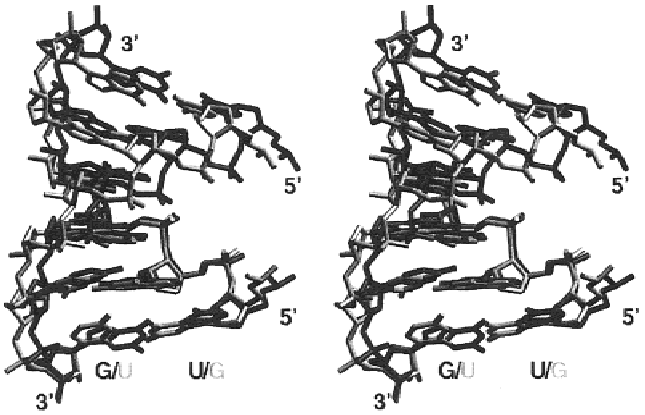

FIGURE 10. Side-by-side stereo representation of two regular Watson–Crick duplexes containing a GoU or a UoG pair (bottom). The C1′ atoms of the riboses involved in the wobble pairs have been superimposed to emphasize the relative deviation of the backbone coordinates.

Crystallization and data collection

Prior to crystallization, the RNA was renatured at a concentration of 10 mg/mL in 5 mM $MgCl_2$ and 10 mM sodium cacodylate, pH 6.0, by heating during 10 min at 85 °C followed by slow cooling to room temperature. One volume of this solution was then mixed with one volume of the reservoir solution (2.2–2.6 M ammonium sulfate, 5–50 mM magnesium sulfate, 50 mM sodium cacodylate, pH 6.0, and 1 mM spermine) on a cover-slip and sealed with vacuum grease on the wells of a Linbro box. Crystals, observed after several days, typically looked like extruded hexagons of regular or irregular geometry with size ranging from 100 to 400 μm.

Four data sets were subsequently collected under cryogenic conditions (110 K), using three different crystals. The first two were collected on a Enraf-Nonius rotating copper anode source operating at 45 kV and 100 mA, coupled to a MacScience detector (dip 2,000), to 1.83 and 1.57 Å resolution, respectively. Data sets were collected to 99.1% and 99.8% completeness, merging to Rsym 3.6% and 3.8%, respectively. A majority of the reflections (>95%) presented I/σ ratios greater than 10 even in the last resolution shells. The third data set, collected on beamline DW32 at the Laboratoire pour l'Utilisation du Rayonnement Électromagnétique (LURE) synchrotron facility using a Mar Research detector (mar 345 cm), was collected to 98.9% completeness at 1.12 Å (Rsym = 3.5%). The distance crystal detector was set to 120 mm with $\lambda = 0.92$ Å. The fourth data set was collected on beamline ID14-EH4 at the European Synchrotron Radiation Facility (ESRF) ($\lambda = 0.934$ Å). The decentering of the CCD camera towards the beam enabled the collection of data to 0.92 Å of resolution, but data were complete enough only to 0.97 Å. Data were processed with the HKL package (Otwinowski & Minor, 1996) in space group R3 for the four crystals. To get a complete data set at high resolution, medium resolution passes were merged with the high resolution passes of the ESRF. The resulting lattice parameters are $a = b = 39.958$ Å, $c = 67.445$ Å, $\gamma = 120°$. The data set consists of 23,838 unique reflections representing a completeness of 99.8% (last shell 99.9%) and the Rsym is 4.1% (last shell 44.6%).

Structure solution and refinement

The structure was solved by the molecular replacement method using the program AMoRe (Navaza, 1994) with the

data set collected to 1.83 Å ($a = b = 39.90$ Å, $c = 67.21$ Å, $\alpha = \beta = 90°$; $\gamma = 120°$). The refinement was completed with the highest resolution data set. We started by searching both strands of a model of the four mismatches exhibited by the three-dimensional model of the SECIS element sandwiched between two C=G or G=C pairs on each side (Walczak et al., 1996). Between 8.0 and 3.5 Å, several solutions were found with correlation factors around 37% and R-factors around 48%. We thought that the backbone distortion in the mismatched region was impeding the molecular replacement process and decided to search two copies of the four 5′ base pairs to give sufficient leeway at the step in the middle of the eight base-pair duplex. This significantly raised the correlation to 52% and lowered the R-factor to 44%. At this time, no modification of the search parameters could improve the solution. The search for two Watson–Crick helices of four random base pairs generated with the program NAHELIX (Westhof, 1993) was then performed as a negative control. Strikingly, the statistics indicated that it was the best solution, with correlation of 66.5% and R-factor of 38.3% in a packing showing no bad contacts.

A rigid-body refinement of a model with correct sequence was performed using CNS (Brünger et al., 1998) and a 3Fo–2Fc map was calculated to inspect the positions of base pairs and phosphate groups at high contour level (3.0 sigma units). All phosphates could be superimposed to a given peak in the map, meaning that the structure of the backbone was basically solved. We then carefully inspected the packing generated from the molecular replacement solution at the step between the two halves of the model. This step adopted a very low twist value, indicating we were considering the junction between two symmetry-related duplexes instead of the step between the two halves of the model. The duplex was then screwed 4 bp along the helical axis to place the apical base pair at the correct step and a new refinement performed, as described above. The decrease observed both for R (33.1%) and R-free (38.6%) was in agreement with the hypothesis. The subsequent inspection of a 2Fo–Fc map indicated that the structure of the backbone was solved whereas the structure of the sequence was wrong.

Because omit maps clearly indicated that the 3′ residue was of the deoxyribose type, we deduced that dC9 and dC18 were, unexpectedly, involved in base pairing. The base-pair scheme could be rearranged by sliding 2 bp in the 5′ direction and the formation of six Watson–Crick and two wobble pairs, resulting in the dangling of the 5′-rC. The model was annealed in CNS, and 41 water molecules were added, decreasing R to 26.6% and R-free to 26.2%. The inspection of a 2Fo-Fc map showed the sequence was right but the dangling 5′-rC could not be seen, meaning it was disordered or hydrolyzed. This question was investigated by MALDI-TOF spectrometry experiments under conditions described elsewhere (Lecchi et al., 1995). The spectra performed with the starting RNA solution exhibit peaks corresponding to the correct nonamer product. A washed and subsequently dissolved crystal yielded peaks corresponding to the correct-length product as well as a 5′-C-pruned product with a 5′-OH end. Because the correct product is synthesized, hydrolysis could intervene during the renaturation process, resulting in the loss of the phosphate group of the first G of the sequence. yet, the removal of the phosphate results in the increase of both R and R-free while its presence in the model contributes correctly to the maps.

The structure was refined to 1.12 Å and then to 0.97 Å with SHELX (Sheldrick & Schneider, 1997) without any σ cut-off for reflections. R-free was composed of 5% of the reflections. R values are communicated for 21,657 reflections with intensity over 4 σ. The refinement started with the naked RNA and yielded an R-factor of 22.51% and an R-free of 25.11%. The identification of a disordered sulfate ion on the threefold axis decreased R and R free to 21.29 and 23.92%, respectively. The addition of 44 water molecules decreased R to 17.57% and R-free to 21.05%. At this stage, R and R-free could be reduced to 16.85% and 20.19% by an anisotropic description of the B factors. The 40 remaining water molecules were added step by step to the model and minor adjustments, including occupancy check of water molecules, led to an R-factor of 14.66% and an R-free of 19.31%. A final cycle of refinement with the 5% of reflections composing the R-free was performed. The final R-factor is 14.81%. The coordinates and the reflection data have been deposited in the Nucleic Acid Database (NDB AR0019).

Computer programs

Model building and electron density map inspections were performed with the O graphical system (Jones et al., 1991). Pictures were prepared with SETOR (Evans, 1993), and DRAWNA (Massire et al., 1994).

ACKNOWLEDGMENTS

B.M. was supported by a Bourse-Docteur-Ingénieur CNRS/Rhône-Poulenc-Rorer and a Human Frontier Science Program grant (to E.W.). C.S. acknowledges a grant from the Ministère de l'enseignement supérieur et de la recherche. Special thanks are due to the Agence Nationale pour la Recherche sur le SIDA (ANRS) for financial help towards the cost of the in-house X-ray generator and detector (grant to Bernard Ehresmann). We are most grateful to P. Dumas for the use of the diffractometer. We acknowledge S. McSweeney and colleagues at ESRF and R. Fourme and the team at LURE for their help during data collection.

Received June 4, 1999; returned for revision July 15, 1999; revised manuscript received July 26, 1999

REFERENCES

Anderson AC, Earp BE, Frederick CA. 1996. Sequence variations as a strategy for crystallizing RNA motifs. *J Mol Biol 259*:696–703.

Antao VP, Tinoco IJ. 1992. Thermodynamic parameters for loop formation in RNA and DNA hairpin tetraloops. *Nucleic Acids Res 20*:819–824.

Arnott S, Hukins DWL, Dover SD, Fuller W, Hodgson AR. 1973. Structures of synthetic polynucleotides in the A-RNA and A′-RNA conformations: X-ray diffraction analyses of conformations of polyadenylic acid-polyuridylic acid and polyinosynic acid-polycydidylic acid. *J Mol Biol 81*:107–122.

Auffinger P, Westhof E. 1997. Rules governing the orientation of the 2′-hydroxyl group in RNA. *J Mol Biol 274*:54–63.

Auffinger P, Westhof E. 1998. Hydration of RNA base pairs. *J Biomol Struct Dyn 16*:693–707.

Baeyens KJ, De Bondt HL, Holbrook SR. 1995. Structure of an RNA double helix including uracil–uracil base pairs in an internal loop. *Nature Struct Biology 2*:56–62.

Baeyens KJ, De Bondt HL, Pardi A, Holbrook SR. 1996. A curved

RNA helix incorporating an internal loop with G·A and A·A non-Watson–Crick base pairing. *Proc Natl Acad Sci USA 93*:12851–12855.
Biswas R, Sundaralingam M. 1997. Crystal structure of r(GUGU GUA)dC with tandem GU/UG wobble pairs with strand slippage. *J Mol Biol 270*:511–519.
Biswas R, Wahl MC, Ban C, Sundaralingam M. 1997. Crystal structure of an alternating octamer r(GUAUGUA)dC with adjacent GU wobble pairs. *J Mol Biol 267*:1149–1156.
Brünger AT, Adams PD, Clore GM, DeLano WL, Gros P, Grosse-Kunstleve RW, Jiang J-S, Kuszewski J, Nilges M, Pannu NS, Read RJ, Rice LM, Simonson T, Warren GL. 1998. Crystallography and NMR system: A new software for macromolecular structure determination. *Acta Cryst D54*:905–921.
Butcher SE, Dieckmann T, Feigon J. 1997. Solution structure of a GAAA tetraloop receptor RNA. *EMBO 16*:7490–7499.
Cate JH, Doudna JA. 1996. Metal binding sites in the major groove of a large ribozyme domain. *Structure 4*:1221–1229.
Cate JH, Gooding AR, Podell E, Zhou K, Golden BL, Kundrot CE, Cech TR, Doudna JA. 1996. Crystal structure of a group I ribozyme domain: Principles of RNA packing. *Science 273*:1678–1684.
Cech TR, Damberger SH, Gutell RR. 1994. Representation of the secondary and tertiary structure of group I introns. *Nature Struct Biol 1*:273–280.
Cech TR, Zaug AJ, Grabowski PJ. 1981. In vitro splicing of the ribosomal RNA precursor of *Tetrahymena*: Involvement of a guanosine nucleotide in the excision of the intervening sequence. *Cell 27*:487–496.
Crick FHC. 1966. Codon-anticodon pairing: The wobble hypothesis. *J Mol Biol 19*:548–555.
Cruse WBT, Saludjian P, Biala E, Strazewski P, Prangé T, Kennard O. 1994. Structure of a mispaired RNA double helix at 1.6-Å resolution and implications for the prediction of RNA secondary structure. *Proc Natl Acad Sci USA 91*:4160–4164.
Egli M, Portmann S, Usman N. 1996. RNA hydration: A detailed look. *Biochemistry 35*:8489–8494.
Evans SV. 1993. SETOR: Hardware-lighted three-dimensional solid model representations of macromolecules. *J Mol Graph 11*:134–138.
Frugier M, Schimmel P. 1997. Subtle atomic group discrimination in the RNA minor groove. *Proc Natl Acad Sci USA 94*:11291–11294.
Holbrook SR, Cheong C, Tinoco I, Kim SH. 1991. Crystal structure of an RNA double-helix incorporating a track of non-Watson–Crick base pairs. *Nature 353*:579–581.
Jones TA, Zou JY, Cowan SW, Kjeldgaard M. 1991. Improved methods for building models in electron density maps and the location of errors in these models. *Acta Cryst A47*:110–119.
Larson SB, Day J, Greenwood A, McPherson A. 1998. Refined structure of satellite tobacco mosaic virus at 1.8-angstrom resolution. *J Mol Biol 277*:37–59.
Lavery R, Sklenar H. 1989. Defining the structure of irregular nucleic acids: Conventions and principles. *J Biomol Struct Dyn 6*:655–667.
Lecchi P, Le HMT, Pannell LK. 1995. 6-Aza-2-thiothymine: A matrix for MALDI spectra oligonucleotides. *Nucleic Acids Res 23*:1276–1277.
Lietzke S, Barnes CL, Berglund JA, Kundrot CE. 1996. The structure of an RNA dodecamer shows how tandem U-U base pairs increase the range of stable RNA structures and the diversity of recognition sites. *Structure 4*:917–930.
Masquida B, Westhof E. 1999. Crystallographic structures of RNA oligonucleotides and ribozymes. In: Neidle S, ed. *Oxford handbook of nucleic acid structures*. Oxford, UK: Oxford University Press. pp 533–565.
Massire C, Gaspin C, Westhof E. 1994. DRAWNA: A program for drawing schematic views of nucleic acids. *J Mol Graph 12*:201–206.
McClain WH, Chen Y-M, Foss K, Schneider J. 1988. Association of transfer RNA acceptor identity with a helical irregularity. *Science 242*:1681–1684.
Michel F, Jaquier A, Dujon B. 1982. Comparison of fungal mitochondrial introns reveals extensive homologies in RNA secondary structure. *Biochimie 64*:867–881.
Michel F, Westhof E. 1990. Modeling of the three-dimensional architecture of group-I catalytic introns based on comparative sequence analysis. *J Mol Biol 216*:585–610.
Mizuno H, Sundaralingam M. 1978. Stacking of Crick wobble pair and Watson–Crick pair: Stability rules of G–U pairs at ends of helical stems in tRNAs and the relation to codon–anticodon wobble interaction. *Nucleic Acids Res 5*:4451–4461.
Mueller U, Schübel H, Sprinzl M, Heinemann U. 1999. Crystal structure of acceptor stem of tRNAAla from *Escherichia coli* shows unique GoU wobble base pair at 1.16 Å resolution. *RNA 5*:670–677.
Musier-Forsyth K, Usman N, Scaringe S, Doudna J, Green R, Schimmel P. 1991. Specificity for aminoacylation of an RNA helix: An unpaired exocyclic amino group in the minor groove. *Science 253*:784–786.
Navaza J. 1994. AMoRe: An automated package for molecular replacement. *Acta Cryst A50*:157–163.
Otwinowski Z, Minor W. 1996. Processing of X-ray diffraction data collected in oscillation mode. *Methods Enzymol 276*:307–326.
Oubridge C, Ito N, Evans PR, Teo C-H, Nagai K. 1994. Crystal structure at 1.92 Å resolution of the RNA-binding domain of the U1A spliceosomal protein complexed with an RNA hairpin. *Nature 372*:432–438.
Park SJ, Hou YM, Schimmel P. 1989. A single base pair affects binding and catalytic parameters in the molecular recognition of a transfer RNA. *Biochemistry 28*:2740–2746.
Pflugrath JW, Quiocho FA. 1985. Sulphate sequestered in the sulphate-binding protein of *Salmonella typhimurium* is bound solely by hydrogen bonds. *Nature 314*:257–260.
Portmann S, Usman N, Egli M. 1995. The crystal structure of r(CCCCGGGG) in two distinct lattices. *Biochemistry 34*:7569–7575.
Rossjohn J, McKinstry WJ, Oakley AJ, Verger AJ, Flanagan J, Chelvanayagam G, Tan KL, Board PG, Parker MW. 1998. Human theta class glutathione transferase: The crystal structure reveals a sulfate-binding pocket within a buried active site. *Structure 6*:309–322.
Scott WG, Finch JT, Grenfell R, Fogg J, Smith T, Gait MJ, Klug A. 1995. Rapid crystallization of chemically synthesized Hammerhead RNAs using a double screening procedure. *J Mol Biol 250*:327–332.
Sharmeen L, Kuo MY-P, Dinter-Gottlieb G, Taylor J. 1988. Antigenomic RNA of human hepatitis delta virus can undergo self-cleavage. *J Virol 62*:2674–2679.
Sheldrick GM, Schneider TR. 1997. High resolution refinement. *Methods Enzymol 276*:307–326.
Shi K, Wahl M, Sundaralingam M. 1999. Crystal structure of an RNA duplex r(GGGCGCUCC)2 with non-adjacent GoU base pairs. *Nucleic Acids Res 27*:2196–2201.
Strobel SA, Ortoleva-Donnelly L. 1999. A hydrogen-bonding triad stabilizes the chemical transition state of a group I ribozyme. *Chem Biol 6*:153–165.
Su L, Chen L, Berger JM, Rich A. 1999. Minor groove RNA triplex in the crystal structure of a ribosomal frameshifting viral pseudoknot. *Nature Struct Biol 6*:285–292.
Wahl MC, Ban C, Sekharudu C, Ramakrishnan B, Sundaralingam M. 1996. Structure of the purine-pyrimidine alternating RNA double-helix, r(GUAUAUA)d(C), with a 3′-terminal deoxy residue. *Acta Cryst D52*:655–667.
Walczak R, Carbon P, Krol A. 1998. An essential non-Watson–Crick base-pair motif in 3′UTR to mediate selenoprotein translation. *RNA 4*:74–84.
Walczak R, Westhof E, Carbon P, Krol A. 1996. A novel RNA structural motif in the selenocysteine insertion element of eukaryotic selenoprotein mRNAs. *RNA 2*:354–366.
Westhof E. 1993. Modeling the three-dimensional structure of ribonucleic acids. *J Mol Struct Dyn 286*:203–210.
Westhof E, Beveridge DL. 1990. Hydration of nucleic acids. In: Franks F, ed. *Water sciences reviews 5: The molecules of life.* Cambridge, United Kingdom: Cambridge University Press. pp 24–136.
Westhof E, Dumas P, Moras D. 1985. Crystallographic refinement of yeast aspartic acid transfer RNA. *J Mol Biol 184*:119–145.
Wu M, Tinoco I. 1998. RNA folding causes secondary structure rearrangement. *Proc Natl Acad Sci USA 95*:11555–11560.
Xiong Y, Sundaralingam M. 1998. Crystal structure and conformation of a DNA–RNA hybrid duplex with a polypurine RNA strand: d((TTCTTBrCTTC)-C-5)-r(GAAGAAGAA). *Structure 6*:1493–1501.